Drug Design, Development and Therapy

Dovepress

open access to scientific and medical research

Open Access Full Text Article

ORIGINAL RESEARCH

Enhancement of Pancreatic Cancer Therapy Efficacy by Type-1 Matrix Metalloproteinase-Functionalized Nanoparticles for the Selective Delivery of Gemcitabine and Erlotinib

This article was published in the following Dove Press journal:
Drug Design, Development and Therapy

Na Yin
Hui Yu
Xiaodi Zhang
Xiaodan Lv

Department of Pharmacy, Jinan Infectious Diseases Hospital Affiliated to Shandong University, Jinan 250000, People's Republic of China

Purpose: Pancreatic cancer (PCa) is projected to become the second leading cause of cancer-related deaths by 2030. Gemcitabine (GEM) combined with erlotinib (ERL) have been approved by the FDA for locally advanced, unresectable or metastatic pancreatic cancer therapy since 2005. Type-1 matrix metalloproteinase (MT1-MMP) has been recognized as a critical mediator of several steps in PCa progression including activating TGF-β or releasing latent TGF-β from LTBP-1, resulting in increased collagen production and cleavage collagen.

Methods: In the present research, GEM and ERL co-loaded nanoparticles (GEM/ERL NPs) were prepared. A non-substrate MT1-MMP binding peptide was decorated onto the GEM/ERL NPs surface.

Results: M-M GEM/ERL NPs exhibited the highest uptake ability (67.65 ± 2.87%), longest half-life period, largest area under the curve, and the best tumor inhibition efficiency (69.81 ± 4.13%). The body weight, blood urine nitrogen (BUN), aspartate aminotransferase (AST), and alanine aminotransferase (ALT) of the system were steady when tested in mice model.

Conclusion: In conclusion, M-M GEM/ERL NPs protected the drugs in the plasma, improved cellular uptake capacity, exhibited the most remarkable tumor cell inhibition ability, and showed the most efficient tumor growth inhibition capacity in vivo. M-M GEM/ERL NPs could be applied as an efficient and safe system for the synergistic combination chemotherapy of PCa.

Keywords: pancreatic cancer, gemcitabine, erlotinib, type-1 matrix metalloproteinase, lipid nanoparticles

Introduction

Pancreatic cancer (PCa), a highly aggressive lethal neoplasm, is the fourth most common cause of cancer-related deaths in the United States, with a 5-year overall survival rate of 6% to 8% at present; and PCa is projected to become the second leading cause of cancer-related deaths by 2030.[1–3] More than 85% of PCa patients are diagnosed at locally advanced or metastatic stages who are not suitable for surgery but systemic therapy as the primary therapeutic option.[4] Therefore, it is urgent to exploit breakthrough strategies for PCa therapy.

Gemcitabine (GEM) monotherapy is recommended as the gold standard front-line therapy for patients with metastatic disease or locally advanced disease.[5,6]

Correspondence: Xiaodan Lv
Jinan Infectious Diseases Hospital, No. 22029 Jingshi Road, Jinan 250000, People's Republic of China
Email lvxdjidh@tom.com

submit your manuscript | www.dovepress.com
DovePress
http://doi.org/10.2147/DDDT.S270303

However, its therapeutic effect is hampered by its rapid metabolism and drug resistance.[7–9] Therefore, GEM-based combination therapies (gemcitabine plus albumin-bound paclitaxel, gemcitabine plus erlotinib) have been upgraded as a category 1 recommendation for advanced PCa by the NCCN guidelines because of the significant effectiveness and safety results from multiple clinical and experimental investigations.[10–12] Compared with combinations of conventional agents, combinations of GEM and targeted agents are research hotspots, despite facing some challenges, still achieving some progresses that deserve further investigation.[13–15] In this study, we devoted ourselves to engineering smart nanocarriers to co-deliver GEM and erlotinib (ERL) for PCa therapy.

Gemcitabine, 2′-deoxy-2′,2′-difluorocytidine, is a broad-spectrum antitumor drug with short half life of 8 to 17 min and hydrophilic property.[13] Erlotinib is an epidermal growth factor receptor (EGFR) tyrosine kinase inhibitor, and EGFR is overexpressed in up to 95% of pancreatic tumors.[16] ERL combined with GEM have been approved by the FDA for locally advanced, unresectable or metastatic pancreatic cancer therapy since 2005.[17] However, ERL is a hydrophobic drug and has several dose-limiting side effects such as rashes, mucositis, anemia, etc.[18] Therefore, it is important to design a drug delivery system to co-deliver a hydrophilic drug (GEM) and a hydrophobic drug (ERL) with lower effective drug content, coordinated drug release and less side effects.

Stimulus-responsive nanoparticles co-deliver drugs at the target tumor zones, effectively minimizing drug administration dosage and enhancing the therapeutic benefits and safety.[19] Matrix metalloproteinases (MMPs) proteolytic enzymes are over-expressed in various types of tumors including PCa.[20–22] Recent studies have indicated that MMP-9 outlayer of MMP-9 responsive nanoparticles can act as a trigger by employing enzyme-responsive peptides.[20,23] Compared with MMP-9 (an anti-target), type-1 matrix metalloproteinase (MT1-MMP) has been recognized as a critical mediator of several steps in PCa progression including activating TGF-β or releasing latent TGF-β from LTBP-1, resulting in resulted in increased collagen production and hence an increased fibrotic microenvironment.[24] Thus, MT1-MMP plays a key role in establishing the desmoplastic reaction in pancreatic cancer.[25] Examples included a non-substrate MT1-MMP binding peptide (MT1-AF7p) conjugated nanoparticles were developed and act on glioma cells.[26] Targeting MT1-MMP has been proposed to sensitize PCa to GEM in vivo.[27] A non-substrate MT1-MMP binding peptide functionalized, GEM and ERL co-loaded nanoparticles (M-M GEM/ERL NPs) were designed in this study.

In the present research, GEM and ERL co-loaded nanoparticles (GEM/ERL NPs) were prepared. A non-substrate MT1-MMP binding peptide was decorated onto the GEM/ERL NPs surface. M-M GEM/ERL NPs exhibited the highest uptake ability (67.65 ± 2.87%), longest $T_{1/2}$, largest AUC, and the best tumor inhibition efficiency (69.81 ± 4.13%). Taken the steady body weight, BUN, AST, and ALT of the system tested in mice model, M-M GEM/ERL NPs could be applied as an efficient and safe system for the synergistic combination chemotherapy of PCa.

Materials and Methods

Materials

Glycerol monostearate (GMS) was purchased from Aladdin Industrial Corporation (Shanghai, China). Dulbecco's Modified Eagle's medium (DMEM) was provided by ThermoFisher Scientific (Shanghai, China). GEM, ERL, and Coumarin 6 (C6) were obtained from Sigma-Aldrich China (Shanghai, China). MT1-AF7p (HWKHLHNTKTFLC) was synthesized by ChinaPeptides Co., Ltd (Shanghai, China). Roswell Park Memorial Institute (RPMI 1640) medium, fetal bovine serum (FBS), and 3-(4,5-dimethyl-2-thiazolyl)-2,5-diphenyl-2-H-tetrazolium bromide (MTT) were purchased from Invitrogen Corporation (Carlsbad, CA). DSPE-PEG_{5000}-Maleimide (PEG-DSPE-Maleimide) was provided by Ponsure Biological (Shanghai, China).

The human pancreatic cancer cell lines PANC-1 and AsPC-1 were purchased from American Type Culture Collection (ATCC, Manassas, VA). PANC-1 cells were cultured in DMEM and AsPC-1 cells grown in RPMI 1640 medium supplemented with 10% fetal bovine serum, 100 U/mL penicillin, and 100 μg/mL streptomycin.[28] Cells were cultivated in a humidified incubator at 37°C and 5% CO_2.

Female Wistar rats (240–260 g) and female BABL/c mice (18–22 g) were obtained from Shandong University Laboratory Animal Center (Ji'nan, China). PANC-1 cells (10^6) were injected subcutaneously in the dorsal skin of BABL/c mice to obtain the pancreatic cancer xenograft mouse models. Animals are maintained and treated in compliance with the policy of the National Institutes of Health guide for the care and use of laboratory animals

and the animal experiments were approved by the Medical Ethics Committee of Jinan Infectious Diseases Hospital.

Preparation of GEM and ERL Co-Loaded Nanoparticles

GEM and ERL co-loaded nanoparticles (GEM/ERL NPs) were prepared by an emulsion-evaporation and low temperature-solidification method.[29] Briefly, GMS (100 mg), PEG-DSPE-Maleimide (100 mg), GEM (20 mg), and ERL (20 mg) were dissolved in ethanol (10 mL) and warmed to 75°C under stirring (400 rpm) to form lipid phase. Tween 80 (0.5%, w/v) was dissolved in distilled water (50 mL, 75°C) to achieve the aqueous phase. Then, the lipid phase was dispersed into the aqueous phase under continuous stirring at 400 rpm for 4 h. After the organic solvent was removed, the hot nanoemulsion was dispersed rapidly into 50 mL of cold distilled water (0–2°C) with stirring at 600 rpm for 1.5 h.

Single GEM or ERL loaded nanoparticles (GEM NPs or ERL NPs) were prepared by the same method using one drug only.

Synthesis of M-M GEM/ERL NPs

M-M GEM/ERL NPs (Figure 1) were synthesized by conjugating MT1-AF7p to the surface of GEM/ERL NPs: The sulfhydryl of cysteine in the HWKHLHNTKTFLC amino acid sequence was conjugated to the Maleimide of PEG-DSPE-Maleimide.[23] GEM/ERL NPs (300 mg) were stirred (400 rpm) in distilled water, and then MT1-AF7p (100 mg) were added to the nanoparticles suspension and stirred (400 rpm) for 24 h at 20°C. The obtained M-M GEM/ERL NPs were concentrated and simultaneously purified with several washes with distilled water, and then characterized using ^{1}H-NMR and FTIR methods.

Blank MT1-AF7p functionalized nanoparticles (Blank M-M NPs) were prepared by the same method using no drug. C6 loaded all kinds of nanoparticles were prepared by the same method of adding C6 (25 mg) into each formulation along with the drugs.

MT1-AF7p Density on NPs Surface

MT1-AF7p level on the M-M GEM/ERL NPs surface was determined via a Bicinchoninic acid (BCA) Protein Assay, using undecorated GEM/ERL NPs at the same concentration as the blank control.[26] M-M GEM/ERL NPs and GEM/ERL NPs resuspended in PBS (pH 7.4) were added into a 96-well plate (20 mL per well) and incubated with BCA Protein Assay Reagent (160 mL) at 37°C for 1 h, respectively. Then, the absorption was measured via at 562 nm. The conjugation efficiency (CE) was calculated by the equation: CE (%) = weight of MT1-AF7p on the NPs' surface/weight of total MT1-AF7p added × 100.

MT1-AF7p surface density was calculated by dividing the number of MT1-AF7p molecules by the calculated average number (AN) of NPs by the equation: AN = 6 × weight of NPs/(π × NPs' diameter^{3} × NPs' weight per volume unit).

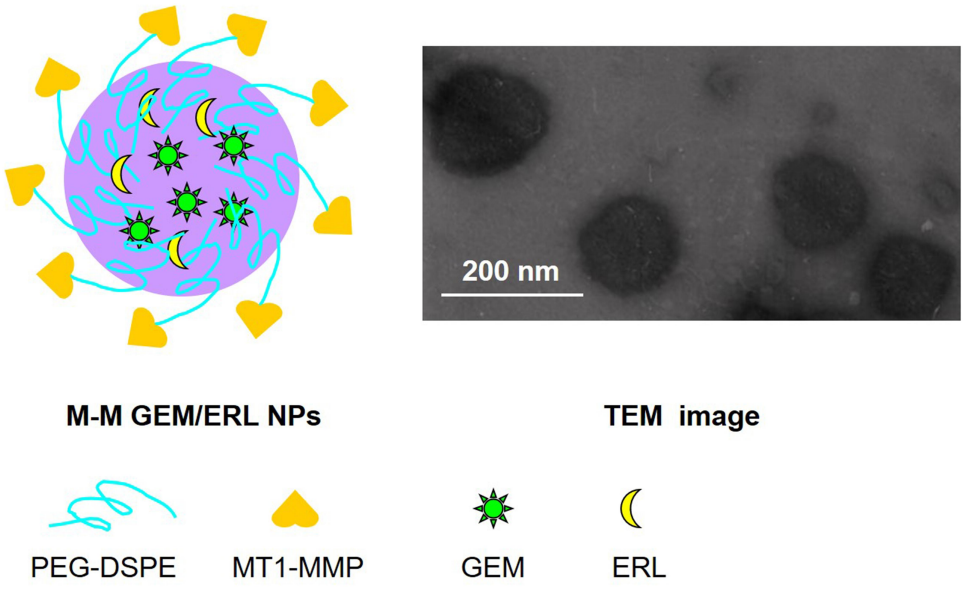

Figure 1 Schematic diagram and TEM image of M-M GEM/ERL NPs. M-M GEM/ERL NPs was synthesized by conjugating MT1-MMP to the surface of GEM/ERL NPs and exhibited uniform spherical morphology.

Characterization of M-M GEM/ERL NPs

The morphology of M-M GEM/ERL NPs was examined by transmission electronic microscopy (TEM) using a JEM-1200EX microscope (JEOL Co., Ltd., Tokyo, Japan).[30] A drop of M-M NPs was placed onto a 200-mesh copper grid and air drying, followed by negative staining with one drop of 3% aqueous solution of sodium phosphotungstate and examined under the TEM. The mean particle size, polydispersity index (PDI), and zeta potential of M-M GEM/ERL NPs was measured using a Zetasizer Nano S90 Nanometer (Malvern, Worcestershire, UK).[31] Samples were diluted to suspensions (1 mg/mL) and tested at 25°C.

Determination of Drug Loading Capacity

Drug loading (DL) and encapsulation efficiency (EE) were calculated by the equations: (1) DL (%) = weight of drugs in NPs/weight of NPs × 100; (2) EE (%) = weight of drugs in NPs/weight of initial drugs added × 100.[32] The amount of GEM was measured by HPLC analysis with an UV detector operated at 248 nm, using methanol as mobile phase (flow rate 1 mL/min) and a C18 column (5 μm, 4.6 mm × 150 mm).[33] The amount of ERL was determined using UV-vis spectrophotometry by measuring the absorbance values at 346 nm.

Plasma Stability

The plasma stability of NPs was evaluated by incubating the samples with FBS at 37°C for 72 h.[34] At determined time points, samples were taken out, the size and EE variations were monitored and the changes were recorded.

In vitro Drug Release

A dialysis method was applied to determine the release behavior of drugs from NPs.[35] Samples were dispersed in PBS at 37°C, sealed in dialysis bags (MWCO: 12 kDa) and immersed in PBS with continuous shaking at 100 rpm. At determined time points, the dialysate (100 μL) was collected and replenished with the same amount of fresh PBS. The amount of drugs was tested by the methods described in "Determination of drug loading capacity" section.

Cellular Uptake

C6 loaded NPs were applied to determine the cellular uptake efficiency.[36] C6 contained NPs (200 mg/mL) were added to the AsPC-1 cells and incubated for 1 h. Then, cells were equilibrated with Hank's buffered salt solution (HBSS) at 37°C for 1 h. The medium was removed after incubated for the determined time, and the wells were washed three times with cold PBS solution and detached with trypsin/EDTA. Cellular uptake efficiency was captured using an inversion fluorescence microscope (OLYMPUS, Tokyo, Japan) and quantified by a FACSCalibur flow cytometer (BD Biosciences, San Jose, CA).

In vitro Cell Viability

PANC-1 and AsPC-1 cells were seeded in 96-well plates (10^4 cells per well) and 100 μL of culture medium containing 10% of NPs or free drugs was added to each well. Cell viability was determined by the MTS CellTiter96® Aqueous Non-Radioactive Cell Proliferation Assay.[37] Briefly, MTS solution (40 μL) was added to each well, and the plates were incubated at 37°C for 3 h. The optical density values were measured at 492 nm after gentle agitation using a multi-well scanning spectrophotometer.

Pharmacokinetics

Female Wistar rats were randomly placed into 3 groups (10 for each group) and intravenously injected with M-M GEM/ERL NPs, GEM/ERL NPs and free GEM/ERL (at GEM dose of 10 mg/kg and ERL dose of 10 mg/kg), respectively.[38] Blood samples (300 μL) were obtained from the tail vein in heparinized tubes at the predetermined time points and the plasma was collected from centrifugation at 10,000 rpm for 10 min. The supernatant was removed, filtered through a 0.2 μm pore size syringe filter and analyzed by the methods described in "Determination of drug loading capacity" section.

In vivo Tumor Growth Inhibition and Toxicity

Pancreatic cancer xenograft mouse models were randomly assigned into 6 groups (10 for each group), and intravenously injected M-M GEM/ERL NPs, GEM/ERL NPs, GEM NPs, ERL NPs, free GEM/ERL (with GEM dose of 10 mg/kg and ERL dose of 10 mg/kg), blank NPs, and 0.9% saline, respectively.[39] The injections were performed every three days for 4 times. Tumor volumes (TV) were measured every three days and calculated by the equation: TV = (the larger perpendicular diameter ×the smaller perpendicular^2)/2. Body weight of each mouse was recorded every three days. To test whether hepatic and renal dysfunctions were induced after administration,

blood was drawn from the venous plexus of the eyes of the mice 24 h after the final injection. Blood samples were immediately centrifuged at 3,000 g for 5 min at 4°C, and the supernatant blood serums were collected for hematological analysis. Blood urine nitrogen (BUN), aspartate aminotransferase (AST), and alanine aminotransferase (ALT) values were measured.

Statistical Analysis

Statistical analysis was performed by Student's *t*-test between two groups, and one-way analysis of variance (ANOVA) among multiple groups. Data are presented as mean ± standard deviation (SD) and statistically significant were confirmed when $P < 0.05$, marking with an asterisk (*).

Results

Characterization of M-M GEM/ERL NPs

M-M GEM/ERL NPs exhibited uniform spherical morphology in Figure 1. ^{1}H NMR spectrum M-M GEM/ERL NPs was shown in Supplement-Figure 1. The peak at about 3.6 ppm stands for the protons of PEG. Peaks at around 1.8 belong to DSPE chain. The chemical shift at 7.0–9.0 ppm is assigned to MT1-AF7p. FTIR spectrum (Supplement-Figure 2) illustrated the new absorption peak at 2865 cm^{-1} for M-M GEM/ERL NPs (Supplement-Figure 2B), which suggested that the MT1-AF7p had been conjugated to GEM/ERL NPs (Supplement-Figure 2A). MT1-AF7p conjugation efficiency was 31.3 ± 2.9%, and the MT1-AF7p peptide density on the nanoparticle surface was 335 ± 31. M-M GEM/ERL NPs showed an increased size (167.82 ± 5.34 nm) than GEM/ERL NPs (123.51 ± 4.66 nm), which may be the evidence that MT1-AF7p decoration enlarged the size (Table 1). Similar sizes were achieved by blank M-M NPs and M-M GEM/ERL NPs, proving the drugs loaded within NPs did not affect the diameter. The zeta potential of M-M GEM/ERL NPs (20.13 ± 2.24 mV) increased compared with GEM/ERL NPs (14.21 ± 1.92 mV), this phenomenon may be explained by the positive charge of MT1-AF7p.

Plasma Stability

Size and EE would not change during the test if the NPs systems are stable in the presence of plasma (Figure 2). During the 72 h of stability study, the particle sizes, GEM and ERL EEs of nanocarriers exhibited negligible changes. These results suggested that these systems could protect the drugs in the plasma and stable during the administration period.

In vitro Drug Release

M-M GEM/ERL NPs and GEM/ERL NPs showed sustained but different release profiles during this experiment (Figure 3). Slower release pattern of M-M GEM/ERL NPs than that of GEM/ERL NPs may be the evidence of the surface coating of peptide which hindered the release of drugs. Drug release behaviors of single drug encapsulated GEM NPs and ERL NPs were similar with dual drugs loaded GEM/ERL NPs.

Cellular Uptake

Cell images showed improved uptake capacity of M-M GEM/ERL NPs than GEM/ERL NPs (Figure 4A). To further determine the cellular uptake efficiency, flow cytometry was applied (Figure 4B). MT1-AF7p decorated M-M GEM/ERL NPs exhibited higher uptake ability (67.65 ± 2.87%) than GEM/ERL NPs (43.17 ± 2.37%) ($P < 0.05$).

In vitro Cell Viability

In vitro cell viability of NPs was evaluated on two kinds of pancreatic tumor cell lines: PANC-1 and AsPC-1 cells (Figure 5). M-M GEM/ERL NPs illustrated the most

Table 1 Characterization of NPs

Formulation	GEM/ERL NPs	GEM NPs	ERL NPs	M-M GEM/ERL NPs	Blank M-M NPs
Particle size (nm)	123.51 ± 4.66	120.93 ± 5.01	125.4 ± 4.37	167.82 ± 5.34*	165.43 ± 5.27
Polydispersity index	0.16 ± 0.03	0.15 ± 0.02	0.14 ± 0.02	0.20 ± 0.03	0.19 ± 0.03
Zeta potential (mV)	14.21 ± 1.92	13.17 ± 2.06	15.32 ± 1.89	20.13 ± 2.24*	19.85 ± 2.17
GEM DL (%)	5.15 ± 0.48	5.29 ± 0.43	/	4.97 ± 0.52	/
ERL DL (%)	5.37 ± 0.61	/	5.21 ± 0.55	4.88 ± 0.42	/
GEM EE (%)	81.31 ± 2.98	80.93 ± 2.37	/	83.14 ± 3.32	/
ERL EE (%)	79.64 ± 2.81	/	81.13 ± 2.59	80.35 ± 3.57	/

Notes: Data are presented as Mean ± SD, n = 10; *P < 0.05 by Student's *t*-test between M-M GEM/ERL NPs and GEM/ERL NPs.

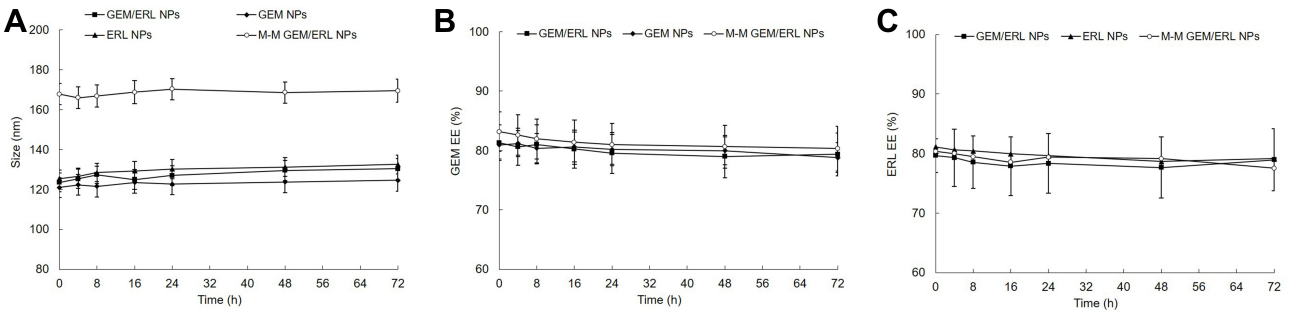

Figure 2 Plasma stability of NPs characterized by the changes of size (**A**), GEM EE (**B**), and ERL EE (**C**). During the 72 h of stability study, the particle sizes, GEM and ERL EEs of nanocarriers exhibited negligible changes. Data are presented as mean ± standard deviation (n=10).

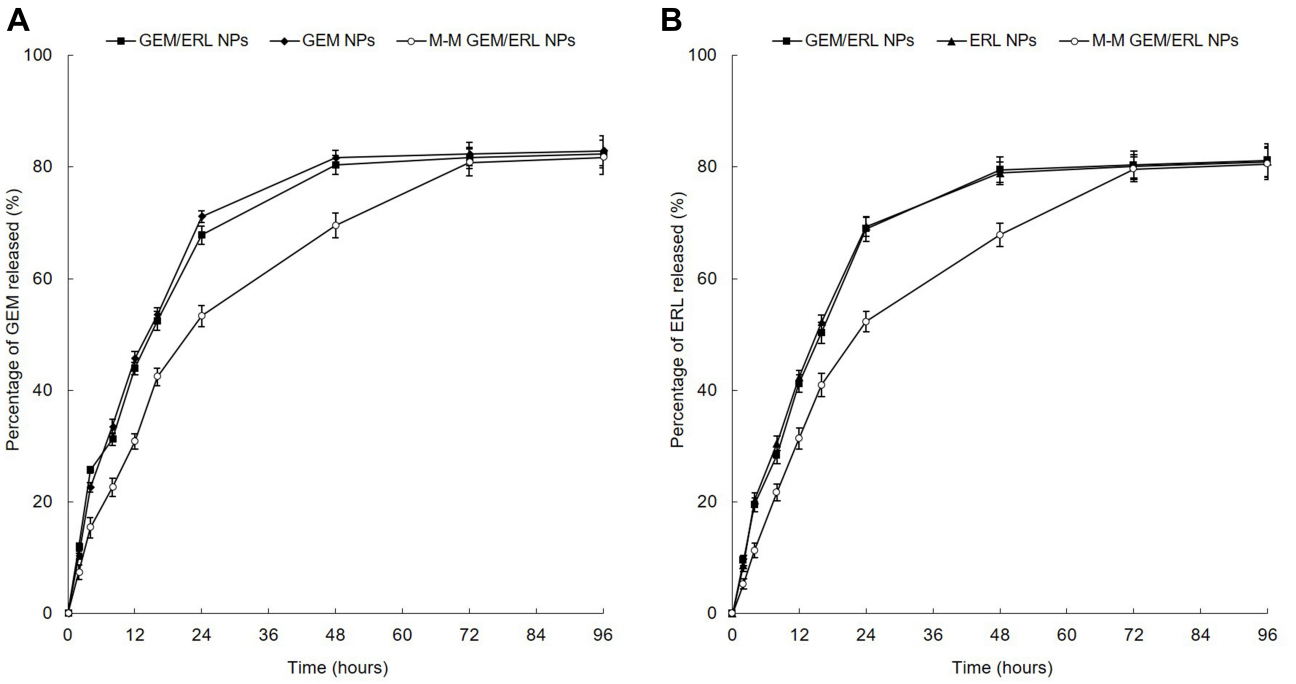

Figure 3 In vitro GEM (**A**) and ERL (**B**) release profiles. M-M GEM/ERL NPs showed slower release than GEM/ERL NPs. The drug release behaviors of single drug encapsulated GEM NPs and ERL NPs were similar with dual drugs loaded GEM/ERL NPs. Data are presented as mean ± standard deviation (n=10).

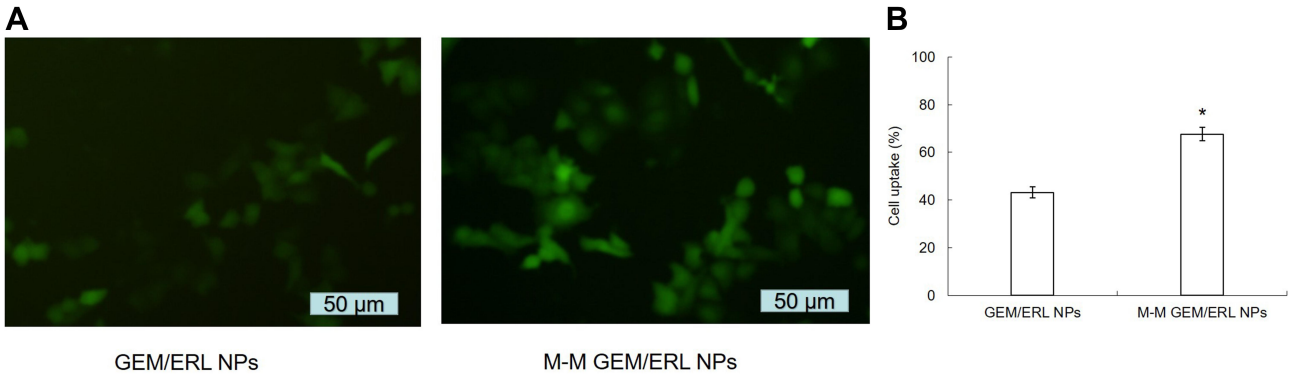

Figure 4 Cellular uptake efficiency of M-M GEM/ERL NPs and GEM/ERL NPs: cell images (**A**) and flow cytometry (**B**). *P < 0.05 compared with GEM/ERL NPs. MT1-MMP decorated M-M GEM/ERL NPs exhibited higher uptake ability (67.65 ± 2.87%) than GEM/ERL NPs (43.17 ± 2.37%). Data are presented as mean ± standard deviation (n=10).

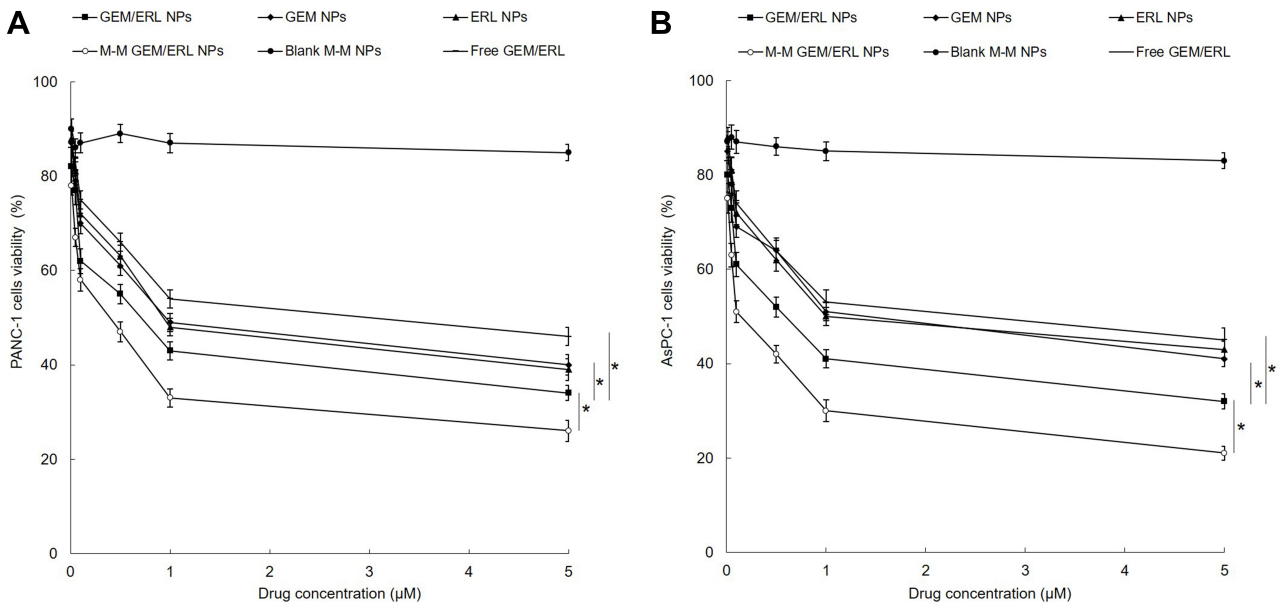

Figure 5 In vitro cell viabilities of NPs evaluated on two kinds of pancreatic tumor cell lines: PANC-1 (**A**) and AsPC-1 cells (**B**). M-M GEM/ERL NPs illustrated the most remarkable tumor cell inhibition ability on both cell lines. GEM/ERL NPs exhibited significantly higher cell inhibition efficiency than free GEM/ERL. Single drug-loaded GEM NPs and ERL NPs showed higher cell viability than their double drugs GEM/ERL NPs counterparts. Data are presented as mean ± standard deviation (n=10). *P < 0.05.

remarkable tumor cell inhibition ability on both cell lines than other groups ($P < 0.05$). GEM/ERL NPs exhibited significantly higher cell inhibition efficiency than free GEM/ERL ($P < 0.05$). Single drug loaded GEM NPs and ERL NPs showed higher cell viability than their double drugs GEM/ERL NPs counterparts ($P < 0.05$), indicating the synergistic cellular inhibition capacity of the two drugs.

Pharmacokinetics

Pharmacokinetics data are summarized in Table 2. M-M GEM/ERL NPs and GEM/ERL NPs showed prominently higher area under the curve, and half-life period than free GEM/ERL. Take GEM data as examples, the $T_{1/2}$, C_{max} and AUC of M-M GEM/ERL NPs were 11.51 ± 1.23 h, 25.17 ± 2.66 L/kg/h, and 106.92 ± 4.64 mg/L h. Compared with the $T_{1/2}$ (1.29 ± 0.34) and AUC (39.45 ± 2.37) of free GEM/ERL, significant improvement (prolonged time and larger AUC) were achieved by the system we constructed ($P < 0.05$).

In vivo Tumor Growth Inhibition and Toxicity

The tumor growth inhibition was evaluated in mice bearing pancreatic tumor models. M-M GEM/ERL NPs group showed the most efficient tumor growth inhibition, and

Table 2 Pharmacokinetics Data

Drug	Formulation	GEM/ERL NPs	M-M GEM/ERL NPs	Free GEM/ERL
GEM	$T_{1/2}$ (h)	8.31 ± 0.92*	11.51 ± 1.23*	1.29 ± 0.34
	C_{max} (L/kg/h)	23.94 ± 2.13	25.17 ± 2.66	20.68 ± 1.95
	AUC (mg/L h)	86.74 ± 3.33*	106.92 ± 4.64*	39.45 ± 2.37
	Vd (L/kg)	3.31 ± 0.51	4.12 ± 0.44	1.21 ± 0.36
	CL (L/h)	0.20 ± 0.03	0.34 ± 0.05	0.65 ± 0.04
ERL	$T_{1/2}$ (h)	9.63 ± 0.86*	12.41 ± 1.53*	1.91 ± 0.78
	C_{max} (L/kg/h)	17.65 ± 1.83	19.32 ± 1.49	18.32 ± 1.73
	AUC (mg/L h)	76.95 ± 4.68*	113.65 ± 7.14*	29.53 ± 3.16*
	Vd (L/kg)	3.81 ± 0.41	4.98 ± 0.47	1.39 ± 0.33
	CL (L/h)	0.27 ± 0.05	0.28 ± 0.04	0.50 ± 0.06

Notes: Data are presented as Mean ± SD, n = 10; *P < 0.05 by Student's *t*-test between M-M GEM/ERL NPs and Free GEM/ERL, or GEM/ERL NPs and Free GEM/ERL.

GEM/ERL NPs also suppressed tumor growth effectively compared to GEM NPs, ERL NPs and free GEM/ERL ($P < 0.05$) (Figure 6). About 70% of tumor inhibition efficiency (69.82%) was achieved by M-M GEM/ERL NPs group, which is higher than that of GEM/ERL NPs (44.04%) and other groups ($P < 0.05$). No obvious body weight change was found (data not shown), indicating there are no serious toxicity of the NPs systems. Little elevation of BUN, AST, and ALT in blood serum was found on NPs groups, and all parameter values were in the normal range (Table 3). However, free drugs group caused an increase in BUN.

Table 3 BUN, AST, and ALT Measurement

Formulation	BUN (mg/dl)	AST (U/L)	ALT (U/L)
GEM/ERL NPs	29.51 ± 1.88	121.6 ± 8.63	75.42 ± 7.32
GEM NPs	31.17 ± 2.15	126.5 ± 9.14	73.13 ± 6.56
ERL NPs	28.76 ± 1.65	130.4 ± 11.16	70.39 ± 8.64
M-M GEM/ERL NPs	27.65 ± 2.77	128.3 ± 7.61	76.34 ± 10.63
Blank M-M NPs	26.88 ± 2.01	120.7 ± 6.59	79.85 ± 9.35
Free GEM/ERL	42.74 ± 2.35 *	136.9 ± 17.32	80.23 ± 12.31

Notes: Data are presented as Mean ± SD, n = 10; *P < 0.05 by Student's *t*-test between Free GEM/ERL and M-M GEM/ERL NPs.

Discussion

Matrix metalloproteinases (MMPs) are major extracellular enzymes that have been detected in cancer; elevated MMP levels have been associated with tumor progression and invasiveness and are widely used as cancer therapeutic targets.[40] Recently, MMPs have been investigated as robust tumor microenvironmental stimuli for "smart" MMP-responsive drug delivery and tumor targeting and have shown great potential in cancer diagnosis and therapy.[41] For example, Ren and colleagues find the efficiency of a MT1-MMP-targeting peptide in near-infrared fluorescence tumor imaging.[42] Morcillo et al using MT1-MMP as an imaging biomarker for pancreas cancer.[43] MT1-MMP has been recognized as a critical mediator of several steps in pancreatic cancer progression and the targeting of MT1-MMP for pancreatic cancer therapeutic intervention can cause significant toxicities.[44] In this study, GEM/ERL NPs were surface decorated with MT1-AF7p.

There are two major kinds of decoration on the surface of NPs: pre and post decoration, which corresponding to the decoration of the ligands before or after the NPs preparation.[45] Examples included Peeters and colleagues proved that post-pegylated lipoplexes are promising vehicles for gene delivery in RPE cells than pre-pegylated counterparts.[46] Pre- or post-bombesin-decorated nanostructured lipid carriers were designed by Du and Li.[47] They argued that post-decorated NPs performed better for targeted lung cancer combination therapy. So in our study, GEM/ERL NPs were firstly prepared and then MT1-AF7p was decorated onto the NPs after NPs construction.

Enhanced permeability and retention (EPR) effect is caused by the leaky vessels and pores in tumor tissues, thus could be utilized by NPs which could easily deliver drugs to the tumor site.[48] The previous research had

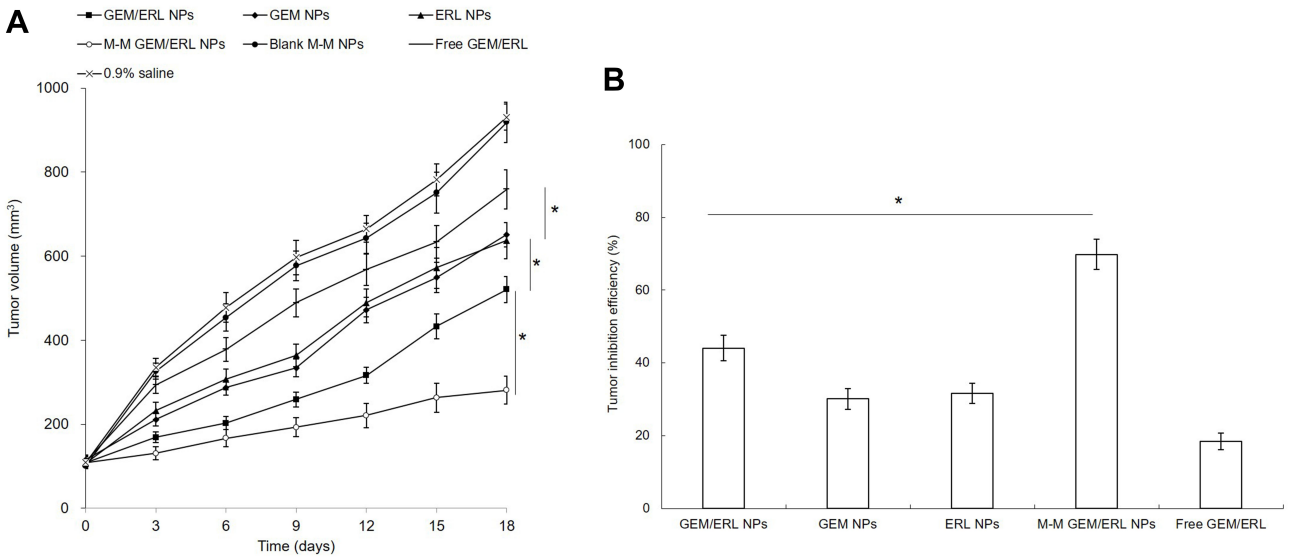

Figure 6 In vivo tumor growth curves (**A**) and tumor inhibition efficiencies (**B**). M-M GEM/ERL NPs group showed the most efficient tumor growth inhibition, and GEM/ERL NPs also suppressed tumor growth effectively compared to GEM NPs, ERL NPs and free GEM/ERL. Data are presented as mean ± standard deviation (n=10). *P < 0.05.

demonstrated that NPs with uniform particle distribution and sizes between 100 and 200 nm could facilitate the delivery of drugs.[49] During the drug delivery after administration, it is critical to maintain stability of the NPs system.[50] The NPs systems were tested in plasma-included media. No obvious changes in size and EE may contribute to the maintenance of stability even in serum-included media.[51]

Nanoparticles could achieve drug depot effects, which would lead to the sustained release of hydrophobic drugs. PEG modification on the surface of nanoparticles could shield the surface from aggregation, opsonization, and phagocytosis, prolonging systemic circulation time.[52] Sustained release behavior of GEM and ERL from NPs could significantly improve the therapeutic efficacy of the drugs loaded.[53] Slower release pattern of M-M GEM/ERL NPs than that of GEM/ERL NPs may be the evidence of the surface coating of peptide which hindered the release of drugs.

Cellular uptake research could provide some circumstantial evidence to display the advantages of the NPs to enter the cancer cells.[54] Higher uptake efficiency of M-M GEM/ERL NPs could be attributed to enhanced cancer cell-specific adherence of the MT1-AF7p. The improved activity and penetration of drugs delivered with NPs can be made use of to improve the efficacy of the standard drug dose, attenuate side effect, and overcome drug resistance. Undecorated GEM/ERL NPs also showed high uptake ability, which suggests that the lipid NPs may have the adherence ability with the cell membrane due to the similar nature of the lipids with the cell membrane.[55] This characteristic could enhance the intracellular drug accumulation and exhibit better anticancer efficiency. In vitro cell viabilities of NPs were evaluated on PANC-1 and AsPC-1 cells. Results showed that the drugs loaded NPs and free drugs reduced cell viability in a concentration-dependent manner.[56] Higher cytotoxicity of the drug-loaded NPs were better than free drug indicating that NPs delivery systems can enhance the cytotoxicity in vitro.

NPs are useful in drug delivery because they can alter the pharmacokinetics of their associated therapeutics.[57] This was observed in our study that the $T_{1/2}$ and AUC of M-M GEM/ERL NPs and GEM/ERL NPs were significantly greater than free GEM/ERL. The AUC of M-M GEM/ERL NPs were also larger than GEM/ERL NPs. Overall, as expected, NPs systems exhibited prolonged half time and larger AUC of drugs. Based on the appropriate physicochemical properties, sustained drug release behavior, and enhanced tumor cells localization, the potential of NPs for the treatment of PCa was further explored on tumor-bearing mice.[57] M-M GEM/ERL NPs group showed the most efficient tumor growth inhibition with over 70% of tumor inhibition efficiency, which is consistent with the previous in vitro cell viability results and successfully highlighting the advantages of combing the GEM and ERL as well as the MT1-AF7p decoration could be a new selectable system for PCa. Steady body weight, BUN, AST, and ALT indicating the low systemic toxicity of the NPs systems. If this system could be used to treat other cancers and the other usage of this system will be examined in the further study. Also, the advantage of the post and pre-modified systems may be discussed on the bases of future experiments.

Conclusion

M-M GEM/ERL NPs were designed in this study. M-M GEM/ERL NPs exhibited the highest uptake ability (67.65 ± 2.87%), longest $T_{1/2}$, largest AUC, and the best tumor inhibition efficiency (69.81 ± 4.13%). M-M GEM/ERL NPs protected the drugs in the plasma, improved cellular uptake capacity, exhibited the most remarkable tumor cell inhibition ability, and showed the most efficient tumor growth inhibition capacity in vivo. M-M GEM/ERL NPs could be applied as an efficient and safe system for the synergistic combination chemotherapy of PCa.

Disclosure

The authors report no conflicts of interest for this work.

References

1. Siegel RL, Miller KD, Jemal A. Cancer statistics, 2018. *CA Cancer J Clin*. 2018;68(1):7–30. doi:10.3322/caac.21442
2. Rawla P, Sunkara T, Gaduputi V. Epidemiology of pancreatic cancer: global trends, etiology and risk factors. *World J Oncol*. 2019;10(1):10–27. doi:10.14740/wjon1166
3. Rahib L, Smith BD, Aizenberg R, Rosenzweig AB, Fleshman JM, Matrisian LM. Projecting cancer incidence and deaths to 2030: the unexpected burden of thyroid, liver, and pancreas cancers in the United States. *Cancer Res*. 2014;74(11):2913–2921. doi:10.1158/0008-5472.CAN-14-0155
4. Peixoto RD, Ho M, Renouf DJ, et al. Eligibility of metastatic pancreatic cancer patients for first-line palliative intent nab-paclitaxel plus gemcitabine versus FOLFIRINOX. *Am J Clin Oncol*. 2017;40(5):507–511. doi:10.1097/COC.0000000000000193
5. Oettle H, Post S, Neuhaus P, et al. Adjuvant chemotherapy with gemcitabine vs observation in patients undergoing curative-intent resection of pancreatic cancer: a randomized controlled trial. *JAMA*. 2007;297(3):267–277. doi:10.1001/jama.297.3.267
6. Oettle H, Neuhaus P, Hochhaus A, et al. Adjuvant chemotherapy with gemcitabine and long-term outcomes among patients with resected pancreatic cancer: the CONKO-001 randomized trial. *JAMA*. 2013;310(14):1473–1481. doi:10.1001/jama.2013.279201

7. Shipley LA, Brown TJ, Cornpropst JD, Hamilton M, Daniels WD, Culp HW. Metabolism and disposition of gemcitabine, and oncolytic deoxycytidine analog, in mice, rats, and dogs. *Drug Metab Dispos*. 1992;20(6):849–855.
8. Sun J, Wan Z, Chen Y, et al. Triple drugs co-delivered by a small gemcitabine-based carrier for pancreatic cancer immunochemotherapy. *Acta Biomater*. 2020;106:289–300. doi:10.1016/j.actbio.2020.01.039
9. Sarvepalli D, Rashid MU, Rahman AU, et al. Gemcitabine: a review of chemoresistance in pancreatic cancer. *Critical Reviews™ in Oncogenesis*. 2019;24(2):199–212. doi:10.1615/CritRevOncog.2019031641
10. Von Hoff DD, Ervin T, Arena FP, et al. Increased survival in pancreatic cancer with nab-paclitaxel plus gemcitabine. *N Engl J Med*. 2013;369(18):1691–1703. doi:10.1056/NEJMoa1304369
11. Samanta K, Setua S, Kumari S, Jaggi M, Yallapu MM, Chauhan SC. Gemcitabine combination nano therapies for pancreatic cancer. *Pharmaceutics*. 2019;11(11):pii: E574. doi:10.3390/pharmaceutics11110574
12. Moore MJ, Goldstein D, Hamm J, et al. Erlotinib plus gemcitabine compared with gemcitabine alone in patients with advanced pancreatic cancer: a phase iii trial of the National Cancer Institute of Canada Clinical Trials Group. *J Clin Oncol*. 2007;25(15):1960–1966.
13. Miller AL, Garcia PL, Yoon KJ. Developing effective combination therapy for pancreatic cancer: an overview. *Pharmacol Res*. 2020;155:104740. doi:10.1016/j.phrs.2020.104740
14. Jamshed MB, Munir F, Shahid N, et al. Antitumor activity and combined inhibitory effect of ceritinib with gemcitabine in pancreatic cancer. *Am J Physiol Gastrointest Liver Physiol*. 2020;318(1):G109–G119. doi:10.1152/ajpgi.00130.2019
15. Wang Y, Hu GF, Zhang QQ, et al. Efficacy and safety of gemcitabine plus erlotinib for locally advanced or metastatic pancreatic cancer: a systematic review and meta-analysis. *Drug Des Devel Ther*. 2016;10:1961–1972. doi:10.2147/DDDT.S105442
16. Oliveira-Cunha M, Newman WG, Siriwardena AK. Epidermal growth factor receptor in pancreatic cancer. *Cancers*. 2011;3(2):1513–1526. doi:10.3390/cancers3021513
17. Adamska A, Domenichini A, Falasca M. Pancreatic ductal adenocarcinoma: current and evolving therapies. *Int J Mol Sci*. 2017;18(7):pii: E1338. doi:10.3390/ijms18071338
18. Marslin G, Sheeba CJ, Kalaichelvan VK, Manavalan R, Reddy PN, Franklin G. Poly(D,L-lactic-co-glycolic acid) nanoencapsulation reduces Erlotinib-induced subacute toxicity in rat. *J Biomed Nanotechnol*. 2009;5(5):464–471. doi:10.1166/jbn.2009.1075
19. Fleige E, Quadir MA, Haag R. Stimuli-responsive polymeric nanocarriers for the controlled transport of active compounds: concepts and applications. *Adv Drug Deliv Rev*. 2012;64(9):866–884. doi:10.1016/j.addr.2012.01.020
20. Kulkarni PS, Haldar MK, Nahire RR, et al. Mmp-9 responsive PEG cleavable nanovesicles for efficient delivery of chemotherapeutics to pancreatic cancer. *Mol Pharm*. 2014;11(7):2390–2399. doi:10.1021/mp500108p
21. Himelstein BP, Canete-Soler R, Bernhard EJ, Dilks DW, Muschel RJ. Metalloproteinases in tumor progression: the contribution of MMP-9. *Invasion Metastasis*. 1994;14(1–6):246–258.
22. Bloomston M, Zervos EE, Rosemurgy AS. Matrix metalloproteinases and their role in pancreatic cancer: a review of preclinical studies and clinical trials. *Ann Surg Oncol*. 2002;9(7):668–674. doi:10.1007/BF02574483
23. Grünwald B, Vandooren J, Locatelli E, et al. Matrix metalloproteinase-9 (MMP-9) as an activator of nanosystems for targeted drug delivery in pancreatic cancer. *J Control Release*. 2016;239:39–48. doi:10.1016/j.jconrel.2016.08.016
24. Krantz SB, Shields MA, Dangi-Garimella S, et al. MT1-MMP cooperates with Kras(G12D) to promote pancreatic fibrosis through increased TGF-β signaling. *Mol Cancer Res*. 2011;9:1294–1304. doi:10.1158/1541-7786.MCR-11-0023
25. Knapinska AM, Estrada CA, Fields GB. The roles of matrix metalloproteinases in pancreatic cancer. *Prog Mol Biol Transl Sci*. 2017;148:339–354.
26. Gu G, Gao X, Hu Q, et al. The influence of the penetrating peptide iRGD on the effect of paclitaxel-loaded MT1-AF7p-conjugated nanoparticles on glioma cells. *Biomaterials*. 2013;34(21):5138–5148. doi:10.1016/j.biomaterials.2013.03.036
27. Dangi-Garimella S, Krantz SB, Barron MR, et al. Three-dimensional collagen I promotes gemcitabine resistance in pancreatic cancer through MT1-MMP-mediated expression of HMGA2. *Cancer Res*. 2011;71(3):1019–1028. doi:10.1158/0008-5472.CAN-10-1855
28. Elechalawar CK, Hossen MN, Shankarappa P, et al. Targeting pancreatic cancer cells and stellate cells using designer nanotherapeutics in vitro. *Int J Nanomedicine*. 2020;15:991–1003. doi:10.2147/IJN.S234112
29. Zhang S, Wang J, Pan J. Baicalin-loaded PEGylated lipid nanoparticles: characterization, pharmacokinetics, and protective effects on acute myocardial ischemia in rats. *Drug Deliv*. 2016;23(9):3696–3703. doi:10.1080/10717544.2016.1223218
30. Yu W, Liu C, Ye J, Zou W, Zhang N, Xu W. Novel cationic SLN containing a synthesized single-tailed lipid as a modifier for gene delivery. *Nanotechnology*. 2009;20(21):215102. doi:10.1088/0957-4484/20/21/215102
31. Zhuang B, Du L, Xu H, et al. Self-assembled micelle loading cabazitaxel for therapy of lung cancer. *Int J Pharm*. 2016;499(1–2):146–-155. doi:10.1016/j.ijpharm.2015.12.073
32. Noorani M, Azarpira N, Karimian K, Heli H. Erlotinib-loaded albumin nanoparticles: a novel injectable form of erlotinib and its in vivo efficacy against pancreatic adenocarcinoma ASPC-1 and PANC-1 cell lines. *Int J Pharm*. 2017;531(1):299–305. doi:10.1016/j.ijpharm.2017.08.102
33. Zhu S, Lansakara-P DS, Li X, Cui Z. Lysosomal delivery of a lipophilic gemcitabine prodrug using novel acid-sensitive micelles improved its antitumor activity. *Bioconjug Chem*. 2012;23(5):966–980. doi:10.1021/bc2005945
34. Zhang R, Ru Y, Gao Y, Li J, Mao S. Layer-by-layer nanoparticles co-loading gemcitabine and platinum (IV) prodrugs for synergistic combination therapy of lung cancer. *Drug Des Devel Ther*. 2017;5(11):2631–2642. doi:10.2147/DDDT.S143047
35. Zheng G, Zheng M, Yang B, Fu H, Li Y. Improving breast cancer therapy using doxorubicin loaded solid lipid nanoparticles: synthesis of a novel arginine-glycine-aspartic tripeptide conjugated, pH sensitive lipid and evaluation of the nanomedicine in vitro and in vivo. *Biomed Pharmacother*. 2019;116:109006. doi:10.1016/j.biopha.2019.109006
36. Zhang J, Xiao X, Zhu J, et al. Lactoferrin- and RGD-comodified, temozolomide and vincristine-coloaded nanostructured lipid carriers for gliomatosis cerebri combination therapy. *Int J Nanomedicine*. 2018;13:3039–3051. doi:10.2147/IJN.S161163
37. Vrignaud S, Hureaux J, Wack S, Benoit J-P, Saulnier P. Design, optimization and in vitro evaluation of reverse micelle-loaded lipid nanocarriers containing erlotinib hydrochloride. *Int J Pharm*. 2012;436(1–2):194–200. doi:10.1016/j.ijpharm.2012.06.026
38. Yalcin TE, Ilbasmis-Tamer S, Takka S. Antitumor activity of gemcitabine hydrochloride loaded lipid polymer hybrid nanoparticles (LPHNs): in vitro and in vivo. *Int J Pharm*. 2020;580:119246. doi:10.1016/j.ijpharm.2020.119246
39. Zhang Y, Kim WY, Huang L. Systemic delivery of gemcitabine triphosphate via LCP nanoparticles for NSCLC and pancreatic cancer therapy. *Biomaterials*. 2013;34(13):3447–3458. doi:10.1016/j.biomaterials.2013.01.063
40. Cui N, Hu M, Khalil RA. Biochemical and biological attributes of matrix metalloproteinases. *Prog Mol Biol Transl Sci*. 2017;147:1–73.
41. Yao Q, Kou L, Tu Y, Zhu L. MMP-responsive 'smart' drug delivery and tumor targeting. *Trends Pharmacol Sci*. 2018;39(8):766–781. doi:10.1016/j.tips.2018.06.003

42. Ren L, Wang Y, Zhu L, et al. Optimization of a MT1-MMP-targeting peptide and its application in near-infrared fluorescence tumor imaging. *Sci Rep*. 2018;8(1):10334. doi:10.1038/s41598-018-28493-9
43. Morcillo MÁ, García de Lucas Á, Oteo M, et al. MT1-MMP as a PET imaging biomarker for pancreas cancer management. *Contrast Media Mol Imaging*. 2018;2018:8382148.
44. Yu W, Zhang N. Surface modification of nanocarriers for cancer therapy. *Curr Nanosci*. 2009;5(2):123–134. doi:10.2174/157341309788185370
45. Peeters L, Sanders NN, Jones A, Demeester J, De Smedt SC. Post-pegylated lipoplexes are promising vehicles for gene delivery in RPE cells. *J Control Release*. 2007;121(3):208–217. doi:10.1016/j.jconrel.2007.05.033
46. Du J, Li L. Which one performs better for targeted lung cancer combination therapy: pre- or post-bombesin-decorated nanostructured lipid carriers? *Drug Deliv*. 2016;23(5):1799–1809. doi:10.3109/10717544.2015.1099058
47. Xu Y, Wu H, Huang J, et al. Probing and enhancing ligand-mediated active targeting of tumors using sub-5 nm ultrafine iron oxide nanoparticles. *Theranostics*. 2020;10(6):2479–2494. doi:10.7150/thno.39560
48. Wang J, Su G, Yin X, et al. Non-small cell lung cancer-targeted, redox-sensitive lipid-polymer hybrid nanoparticles for the delivery of a second-generation irreversible epidermal growth factor inhibitor-Afatinib: in vitro and in vivo evaluation. *Biomed Pharmacother*. 2019;120:109493. doi:10.1016/j.biopha.2019.109493
49. Wang G, Wang Z, Li C, et al. RGD peptide-modified, paclitaxel prodrug-based, dual-drugs loaded, and redox-sensitive lipid-polymer nanoparticles for the enhanced lung cancer therapy. *Biomed Pharmacother*. 2018;106:275–284. doi:10.1016/j.biopha.2018.06.137
50. Cao C, Wang Q, Liu Y. Lung cancer combination therapy: doxorubicin and β-elemene co-loaded, pH-sensitive nanostructured lipid carriers. *Drug Des Devel Ther*. 2019;5(13):1087–1098. doi:10.2147/DDDT.S198003
51. Wang J. Combination treatment of cervical cancer using folate-decorated, pH-sensitive, carboplatin and paclitaxel co-loaded lipid-polymer hybrid nanoparticles. *Drug Des Devel Ther*. 2020;14:823–832. doi:10.2147/DDDT.S235098
52. Gao Z, Li Z, Yan J, Wang P. Irinotecan and 5-fluorouracil-co-loaded, hyaluronic acid-modified layer-by-layer nanoparticles for targeted gastric carcinoma therapy. *Drug Des Devel Ther*. 2017;11:2595–2604. doi:10.2147/DDDT.S140797
53. Duan W, Liu Y. Targeted and synergistic therapy for hepatocellular carcinoma: monosaccharide modified lipid nanoparticles for the co-delivery of doxorubicin and sorafenib. *Drug Des Devel Ther*. 2018;12:2149–2161. doi:10.2147/DDDT.S166402
54. Yan J, Wang Y, Zhang X, Liu S, Tian C, Wang H. Targeted nanomedicine for prostate cancer therapy: docetaxel and curcumin co-encapsulated lipid-polymer hybrid nanoparticles for the enhanced anti-tumor activity in vitro and in vivo. *Drug Deliv*. 2016;23(5):1757–1762. doi:10.3109/10717544.2015.1069423
55. Hong Y, Che S, Hui B, et al. Lung cancer therapy using doxorubicin and curcumin combination: targeted prodrug based, pH sensitive nanomedicine. *Biomed Pharmacother*. 2019;112:108614. doi:10.1016/j.biopha.2019.108614
56. Udofot O, Affram K, Smith T, et al. Pharmacokinetic, biodistribution and therapeutic efficacy of 5-fluorouracil-loaded pH-sensitive PEGylated liposomal nanoparticles in HCT-116 tumor bearing mouse. *J Nat Sci*. 2016;2(1):pii: e171.
57. Yugui F, Wang H, Sun D, Zhang X. Nasopharyngeal cancer combination chemoradiation therapy based on folic acid modified, gefitinib and yttrium 90 co-loaded, core-shell structured lipid-polymer hybrid nanoparticles. *Biomed Pharmacother*. 2019;114:108820. doi:10.1016/j.biopha.2019.108820